PHYSICAL REVIEW B **67**, 041301(R) (2003)

Superconductor-quantum dot-superconductor junction in the Kondo regime

Yshai Avishai,[1] Anatoly Golub,[1] and Andrei D. Zaikin[2,3]
[1]*Ilse Katz Center for Nano-Technology, Ben-Gurion University of the Negev, Beer-Sheva, Israel and Department of Physics, Ben-Gurion University of the Negev, Beer-Sheva, Israel*
[2] *Forschungszentrum Karlsruhe, Institut für Nanotechnologie, 76021 Karlsruhe, Germany*
[3]*I.E.Tamm Department of Theoretical Physics, P.N. Lebedev Physics Institute, 117924 Moscow, Russia*
(Received 31 October 2002; published 9 January 2003)

Electron transport between two superconductors through an Anderson impurity in the Kondo regime is investigated within the slave boson mean-field approximation. The current, shot-noise power and Fano factor are displayed versus the applied bias voltage in the subgap region and found to be strongly dependent on the ratio between the Kondo temperature T_K and the superconducting gap Δ. In particular, the *I-V* curve exposes an excess current in the limit $T_K/\Delta \gg 1$.

DOI: 10.1103/PhysRevB.67.041301 PACS number(s): 72.10.−d, 71.27.+a, 74.40.+k

A number of recently developed experimental techniques allow for detailed investigations of electronic transport through atomic-size metallic conductors.[1] Usually, transport properties of such systems are strongly affected by Coulomb interactions. Novel physical effects emerge if electrodes of an atomic-size contact become superconducting. In that case, the mechanism of multiple Andreev reflections[2] (MAR) plays a dominant role being responsible for both dc Josephson effect and for dissipative currents at subgap voltages. Further, possibilities for experimental investigation of an interplay between MAR and Coulomb effects in systems with few conducting channels are provided by recently fabricated superconducting junctions with a weak link formed by a carbon nanotube.[3,4]

Recently, we developed a theory[5] for the study of an *SAS* junction consisting of an interacting quantum dot (*A*) connected to superconducting (*S*) electrodes. It enables the analysis of MAR in superconducting contacts with few conducting channels in the presence of electron-electron interactions. An interplay between MAR and Coulomb effects is responsible for effects such as an interaction-induced shift of the subharmonic gap steps on the *I-V* curve and Coulomb blockade of MAR. The latter may result in a strong suppression of the subgap current through the dot at sufficiently low temperatures.

The combined effect of MAR and electron-electron interactions on the shot noise[6] in superconducting quantum dots was studied in Ref. 7. It was demonstrated that interaction effects can strongly suppress the shot-noise power at subgap voltages. At the same time, the Fano factor (proportional to the ratio of the shot-noise power and the current) was found to be nearly independent of interaction.

Our previous analysis[5,7] was restricted to physical situations outside the Kondo regime implying that all relevant energies in the problem were taken to be much higher than the Kondo temperature $T_K \approx 0$. In the present work, we study the opposite limit of sufficiently *high* Kondo temperatures. This case is relevant, e.g., for junctions composed of carbon nanotubes,[3,4] where the Kondo effect with rather high Kondo temperature $T_K \approx 1.6$ K was recently observed.[8] Properties of superconducting quantum dots in this strong-coupling regime are entirely distinct from those exposed earlier in the limit $T_K \to 0$. On a qualitative level, this difference between weak and strong coupling regimes can be briefly summarized as follows: In the weak-coupling limit (low T_K), although the number of Andreev reflections $n \sim 2\Delta/eV$ may be large at low voltages V, both the current and shot-noise power remain rather weak. This is due to the low effective transparency $\tilde{\Gamma}$ of the junction as a consequence of strong repulsive electron-electron interaction (Coulomb blockade). Large-n processes are therefore damped as $\tilde{\Gamma}^n$. By contrast, in the strong-coupling Kondo regime the effective transmission is much larger and a ballisticlike channel opens up inside the dot. Hence, an interplay between MAR and the Kondo resonance is expected to yield an excess current in the *I-V* curve, similarly to the case of noninteracting ballistic junctions. At very large values of T_K and in the low-voltage limit this current should approach the noninteracting result[9] $I_{AR} = 4e\Delta/h$. Analogously, the shot-noise power is expected to display a pronounced maximum at $V=0$ and should decay as $1/V$ at small bias as is familiar in the standard noninteracting *SNS* junction.[10] Below, we will present a quantitative analysis which fully supports this qualitative physical picture.

The pertinent system is represented by two half planar electrodes (L and R) separated by the line $x=0$, and weakly coupled to a pointlike Anderson impurity A located at the origin. This model is of interest, for instance, in connection with recent experiments[11,12] on semiconductor quantum dots. It was shown there that tunneling takes place through a separate state with features of a Kondo behavior (a tunable Kondo effect).

The system dynamics is governed by the Hamiltonian

$$H = H_L + H_R + H_d + H_t + H_c, \tag{1}$$

in which $H_{L,R}$ are the BCS Hamiltonians of the electrodes which depend on the electron field operators $\psi_{L(R)\sigma}(\mathbf{r},t)$, where $\mathbf{r}=(x,y)$ and $\sigma = \pm$ is the spin index. As in Refs. 5,7 the dot is described as a single-level Anderson impurity A with energy $\epsilon_0 < 0$ and Hubbard repulsion parameter U. In the Kondo regime of interest, here we set $U \to \infty$ and assume $|\epsilon_0|$ to exceed any other energy scale except U. In this case it is convenient to express the dot and the tunneling Hamiltonians H_d and H_t via slave boson (operators $b, b^\dagger$) and slave

fermion (operators $c,c^\dagger$) auxiliary fields.[13] Explicitly, $H_d=\epsilon_0\Sigma_\sigma c_\sigma^\dagger c_\sigma$ and $H_t=\mathcal{T}\Sigma_{j\sigma}c_\sigma^\dagger b\psi_{j\sigma}(\mathbf{0},t)+\text{H.c.}$, where $\mathcal{T}$ is the tunneling amplitude. Finally, the Hamiltonian of the system must also include a term which prevents double occupancy in the limit $U\to\infty$. This term reads $H_c=\lambda(\Sigma_\sigma c_\sigma^\dagger c_\sigma+b^\dagger b-1)$, where λ is a Lagrange multiplier.

Let us now consider the dynamical ''partition function''

$$Z\sim\int\mathcal{D}[F]\exp(i\mathcal{S}), \tag{2}$$

where the path integral is carried out over all fields $[F]$ and the action $\mathcal{S}$ is obtained by integrating the Lagrangian pertaining to the Hamiltonian (1) along the Keldysh contour. The procedure of integrating out the electron fields of the bulk electrodes $\psi_{L(R)\sigma}(\mathbf{r},t)$ was described in details in Ref. 5. As a result, we arrive at the effective action expressed in terms of the Green functions of the bulk superconductors. Our next step is to integrate out the variables corresponding to the Fermi operators $c_\sigma^\dagger$ and c_σ of the dot. The corresponding integral is Gaussian, which yields

$$S_{\text{eff}}=-i\,\text{Tr}\ln\hat{G}^{-1}-\int dt[\hat{\lambda}\sigma_z(\hat{b}\hat{b}-1)]. \tag{3}$$

Here $\hat{\lambda}=(\lambda_1,\lambda_2)$, $\hat{b}=(b_1,b_2)$, and σ_z are diagonal matrices acting in Keldysh space. Similarly to Ref. 5, the inverse propagator $\hat{G}^{-1}$ depends on the Green functions of the electrodes.

In order to describe the Kondo regime we will treat the slave boson fields b_1 and b_2 in Eq. (3) within the dynamical mean-field approximation. Performing the variation of the effective action with respect to $b_{1,2}$ and $\lambda_{1,2}$ and then setting $b_1=b_2=b$ and $\lambda_1=\lambda_2=\lambda$, we arrive at two self-consistency equations that determine the parameters b and λ.

Before presenting these equations let us specify the expression for the inverse propagator $\hat{G}^{-1}$. Performing the standard basis rotation in Keldysh space one finds

$$\hat{G}^{-1}(\epsilon,\epsilon')=\delta(\epsilon-\epsilon')(\epsilon-\tau_z\tilde{\epsilon})+\frac{\Gamma b^2}{2}\tau_z\hat{g}_+(\epsilon,\epsilon')\tau_z, \tag{4}$$

where $\tilde{\epsilon}=\epsilon_0+\lambda$ is the renormalized level position (in the Kondo limit one has $\tilde{\epsilon}\simeq 0$) and $\Gamma\propto\mathcal{T}^2$ is the usual transparency parameter. Here and below, we define $\hat{g}_\pm=\hat{g}_L\pm\hat{g}_R$, where

$$\hat{g}_{L,R}(t,t')=e^{\mp i\varphi(t)\tau_z/2}\int\hat{g}(\epsilon)e^{-i\epsilon(t-t')}\frac{d\epsilon}{2\pi}e^{\pm i\varphi(t')\tau_z/2}, \tag{5}$$

are Keldysh matrix Green functions of left and right electrodes and $\dot{\varphi}/e=V(t)$ is the bias voltage across the dot. The matrix $\hat{g}$ has the standard structure with retarded and advanced Green functions

$$\hat{g}^{R/A}(\epsilon)=\frac{(\epsilon\pm i0)+|\Delta|\tau_x}{\sqrt{(\epsilon\pm i0)^2-|\Delta|^2}}, \tag{6}$$

as diagonal elements $\hat{g}^{R/A}$ and the Keldysh function $\hat{g}^K(\epsilon)=[\hat{g}^R(\epsilon)-\hat{g}^A(\epsilon)]\tanh(\epsilon/2T)$ as the only nonzero (upper) off-diagonal element. The Pauli matrices $\tau_{x,y,z}$ act in Nambu space. The inverse of the matrix (4) is formally performed, leading to a 2×2 Keldysh Green function with three elements,

$$\hat{G}^{R,A}=\left[\left(i\frac{\partial}{\partial t}-\tau_z\tilde{\epsilon}\right)+\frac{\Gamma b^2}{2}\tau_z\hat{g}_+^{R,A}\tau_z\right]^{-1}, \tag{7}$$

$$\hat{G}^K=-\frac{\Gamma b^2}{2}\hat{G}^R\tau_z\hat{g}_+^K\tau_z\hat{G}^A. \tag{8}$$

In order to explicitly write down the self-consistency equations let us introduce the bare Kondo temperature $T_K^0=D\exp[-\pi|\epsilon_0|/(2\Gamma)]$ and define $\Gamma b^2=T_K^0X$, where D is the energy bandwidth. Then our (MFSBA) equations take the form

$$X=-\frac{i\Gamma}{2T_K^0}\text{Tr}\hat{G}^K\tau_z, \tag{9}$$

$$\lambda=\frac{i\Gamma}{8}\text{Tr}[\hat{G}^K\tau_z(g_+^R+g_+^A)+(\hat{G}^R+\hat{G}^A)\tau_z g_+^K]\tau_z, \tag{10}$$

where the trace also includes energy integration. Eq. (9) effectively determines the Kondo temperature (through the parameter X), and reflects the constraint which prevents double occupancy in the limit $U\to\infty$. The second self-consistency Eq. (10) defines the renormalized energy-level position $\tilde{\epsilon}$.

Let us briefly discuss the validity range of the present analysis. The MFSBA is known to encode the Kondo Fermi-liquid behavior at low temperatures. An important parameter here is the ratio between the Kondo temperature and the superconducting gap $t_K\equiv T_K^0/\Delta$.[14–16] For $t_K\gtrsim 1$ a Fermi-liquid behavior is expected. Accordingly, in this regime Eq. (9) should have a nonzero solution $X\neq 0$, which corresponds to nonzero T_K. On the other hand, in the limit of large Δ the only possible solution is a trivial one $b=0$ (and, hence, $T_K=0$).[18] In this case—as it was demonstrated in Ref. 5—the problem can be treated within the dynamical mean-field approximation for the bare Anderson Hamiltonian. Quantitatively, the MFSBA is reliable only for sufficiently large values of t_K. We believe, however, that it can provide useful qualitative information also for moderate values of t_K describing a crossover between the Kondo regime and the Coulomb blockade behavior.[5] It is worth noting here that the applied bias voltage V also attenuates the Kondo resonance and lowers T_K. Hence, for the reliability of the MFSBA in nonequilibrium situations, both Δ and eV should not exceed the Kondo temperature. Attention below is mainly focused on the subgap voltage regime $eV\lesssim\Delta$ in which case t_K appears to be the only relevant parameter.

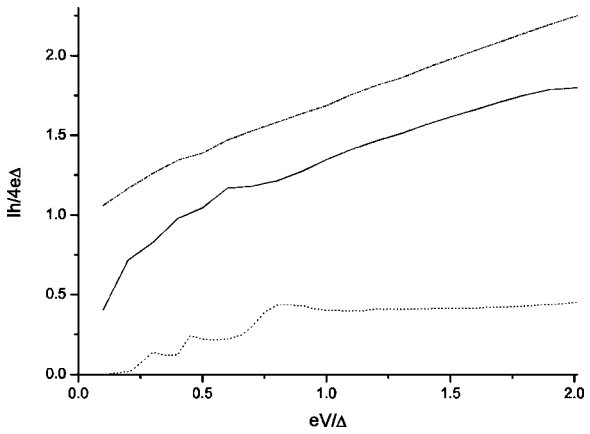

FIG. 1. The averaged current I (in units of $4e\Delta/h$) versus the bias V (in units of Δ/e) for an SAS junction at subgap voltages with $\Gamma/T_K^0=200$. Dashed-dotted, solid, and dotted curves correspond, respectively, to $t_K=100$, 5, and 1.6.

The standard expression[17] for the tunneling current operator between the dot and one (e.g., the right) electrode reads,

$$I_R^{(1,2)}=\pm\frac{ie}{\hbar}\sum_k \mathcal{T}\left[c\frac{1\pm\sigma_x}{2}\psi_{Rk}(0)-\text{H.c.}\right]. \tag{11}$$

Here $\psi_{Rk}(0)$ is the Fourier transform of $\psi_R(0,y,t)$ with respect to y and Eqs. (1) and (2) refer to Keldysh indices. As before, it is convenient to integrate out the ψ fields and express the current I through the dot in terms of the Green functions of the bulk electrodes. This procedure has been described in details in Ref. 5. As a result, we obtain

$$I=i\frac{eXt_K}{8\hbar}\text{Tr}[(\hat{G}^R\tau_z-\tau_z\hat{G}^A)g_-^K-\hat{G}^K\tilde{g}], \tag{12}$$

where we defined $\tilde{g}=\hat{g}_-^R\tau_z-\tau_z\hat{g}_-^A$ and $\tilde{g}^{R,A}=\hat{g}_-^{R,A}\tau_z-\tau_z\hat{g}_-^{R,A}$. Being combined with Eqs. (9) and (10), the result of Eq. (12) can be conveniently used for computing the transport current of an SAS junction in the Kondo regime for different values of t_K.

For sufficiently large t_K, we anticipate a strong Kondo resonance and the I-V curve is expected to resemble that of purely ballistic junctions without interaction.[9] Indeed, in the limit of large $t_K\gg 1$ which corresponds to the unitary, pure ballistic case, our expression for the current (12) reduces to that of Ref. 9. This agreement is further supported by our numerical analysis carried out for $t_K=100$ (dashed-dotted curve in Fig. 1). Calculation of the current was also performed for $t_K=5$ and 1.6 and the results are displayed in Fig. 1. For $t_K=5$, a pronounced excess MAR current is clearly exposed in the I-V curve, though its magnitude turns out to be smaller than in the unitary limit $t_K\gg 1$. One also observes subharmonic MAR steps (which are hardly visible in the case $t_K\gg 1$). For a lower value $t_K=1.6$ the current is strongly suppressed (dotted line in Fig. 1), and the I-V curve resembles that of a low transparency SAS. MAR steps in the I-V curve become more pronounced as compared to the case of higher t_K.

Let us briefly summarize our results for the current. In the limit of large t_K the I-V curve is practically independent of t_K and resembles that of a ballistic junction, as indicated in the upper curve in Fig. 1. This effect is physically similar to that discussed in Refs. 19 and 20, where stimulation of the dc Josephson current was found in the unitary limit of the Kondo regime. For lower values of t_K the junction is driven away from the unitary limit and the system behavior becomes much richer. It reflects the influence of both Δ and V on the Kondo resonance and on the actual value of the Kondo temperature. While for $t_K=5$ some imprint of ballistic behavior still remains (finite excess current), the I-V curve noticeably deviates from that obtained in a noninteracting limit. For $t_K=1.6$ the competition between gap-related suppression of the Kondo effect and the effective transparency of the junction becomes essential leading to further decrease of the current. For even lower values t_K, the Kondo physics is no more relevant and one crosses over to the Coulomb blockade regime.[5]

The shot-noise spectrum is usually defined as the symmetrized current-current correlation function[6]. Being expressed via the operators (11), it reads

$$K(t_1,t_2)=\hbar[\langle\hat{T}I^{(1)}(t_1)I^{(2)}(t_2)\rangle+\langle\hat{T}I^{(1)}(t_2)I^{(2)}(t_1)\rangle-2\langle I\rangle^2], \tag{13}$$

where $\hat{T}$ is the time-ordering operator and $\langle\cdots\rangle$ denotes quantum averaging with the Hamiltonian (1). Substituting $I^{(1,2)}=(I_L^{(1,2)}-I_R^{(1,2)})/2$ into Eq. (13) we obtain an expression for $K(t_1,t_2)$ which involves integration over surface fields and dot electron slave particle field operators. The first integration involving the Green function matrix $\hat{g}$ is Gaussian and can be done exactly. Integrations over the dot slave fermion fields is completed within the dynamic MFSBA. After Fourier transform with respect to t_1-t_2 it is possible to express the power noise spectrum $K(\omega)$ in terms of the Green-functions of the entire system (7) and (8). It is convenient to decompose $K=(K_1+K_2)e^2\Delta/(8\hbar)$ with the result,

$$K_1=\frac{Xt_K}{2}\text{Tr}\{(\hat{g}_+^R-\hat{g}_+^A)(\hat{G}^R-\hat{G}^A)-\hat{g}_+^K\hat{G}^K\}, \tag{14}$$

$$K_2=-\frac{(Xt_K)^2}{8}\text{Tr}\{(\hat{G}^K\tilde{g})^2-2\tau_z\tilde{g}\tau_z\hat{G}^A\tilde{g}\hat{G}^R-[2\tilde{g}\hat{G}^R\tau_z\hat{g}_-^K\hat{G}^K+(\tilde{g}^R\hat{G}^R)^2-(\hat{G}^A\hat{g}_-^K\tau_z)^2+\text{H.c.}]\}. \tag{15}$$

Expressions (14) and (15) [supplemented by the self-consistency Eqs. (9) and (10)] are then solved numerically for the same set of parameters $\Gamma/T_K^0=200$, $t_K=100$, 5, and 1.6. The results for the shot-noise power spectrum K versus the applied voltage V are displayed in Fig. 2. These results are clearly correlated with those for the I-V curve and can be summarized as follows.

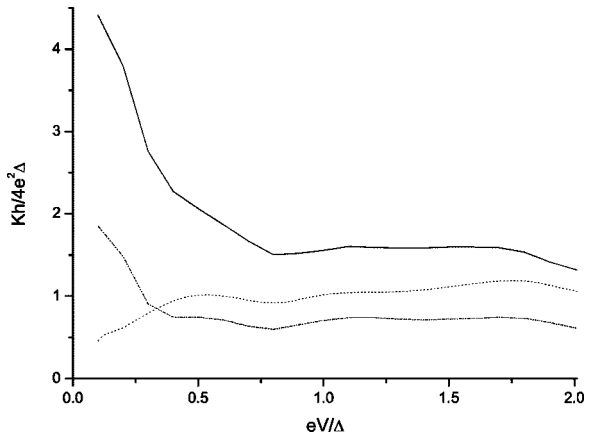

FIG. 2. The shot-noise power K (in units of $2e^2\Delta/h$) as a function of V (in units of Δ/e) for an *SAS* junction. The parameters and notations are the same as in Fig. 1.

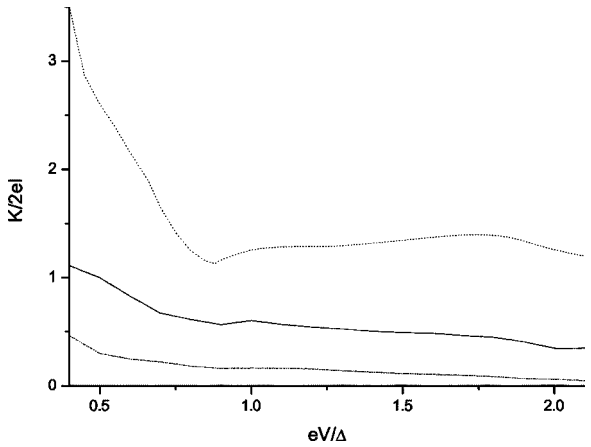

FIG. 3. The Fano factor $K/2eI$ versus V. The parameters and notations are the same as in Fig. 1

In the limit $t_K \gg 1$, our results are consistent with those obtained for purely ballistic junctions.[10] In particular, we mention that the noise spectrum K exhibits a $1/V$ dependence at low voltages. At lower t_K the physics is distinct. For $t_K = 5$ (solid curve) the noise spectrum still shows features typical for a junction with relatively high transparency (see Ref. 21 and Fig. 1 therein), while the results for $t_K = 1.6$ (dotted curve) are more similar to those for a low transparency junction. For $t_K = 5$, we get a pronounced noise power at low voltage whereas at higher voltages $eV \gtrsim \Delta$ the shot noise is significantly suppressed. At low voltage K scales approximately as $1/V$. The sequential tunneling picture is not valid in the unitary limit $t_K \gg 1$ as well as for the intermediate value $t_K = 5$ due to the interference between different MAR processes. Yet, this picture is partially restored at lower Kondo temperatures, as is demonstrated by our results obtained for $t_K = 1.6$. This effect of sequential tunneling due to MAR is most clearly manifested through the Fano factor $K/2eI$ depicted in Fig. 3 as a function V. We observe that for $t_K = 5$ the Fano factor at $eV \gtrsim \Delta$ is substantially lower than the expected value $K/2eI = 2$ originated from Andreev reflections. On the other hand, for $t_K = 1.6$ the Fano factor is closer to this value.

In conclusion, we have analyzed an important physical problem involving strong correlations, the Kondo effect and superconductivity. These aspects can be combined in an *SAS* junction consisting of an Anderson impurity (in the Kondo regime) located between two superconducting electrodes, which is experimentally feasible. We have developed a theoretical framework by which it is possible to investigate an interplay between MAR and Coulomb effects in the Kondo regime $T < \Delta < T_K$. In this limit, we have exposed the nonlinear I-V characteristics and calculated the shot-noise power spectrum of *SAS* junctions at subgap voltages $eV < 2\Delta$. We have found that at sufficiently large t_K the Kondo resonance plays the dominant role effectively making the junction behavior similar to that of highly transparent noninteracting weak links.[9,10] This physical situation is qualitatively different from the Coulomb blockade regime encountered in the limit $\Delta > T > T_K$, which we have analyzed in our previous works.[5,7] A crossover between these two physically different regimes occurs at $T_K \sim \Delta$ and is also—at least qualitatively—described within our theoretical framework.

We would like to thank J. C. Cuevas, D. S. Golubev, L. I. Glazman, J. Kroha and A. Rosch for discussions and useful suggestions. This research is supported by DIP German Israel Cooperation project Quantum electronics in low dimensions by the Israeli Science Foundation grant Many-body effects in nonlinear tunneling and by the US-Israel BSF grant Dynamical instabilities in quantum dots. This work is also a part of the CFN (Center for Functional Nanostructures) supported by the DFG (German Science Foundation).

[1] J.M. van Ruitenbeek, cond-mat/9910394 (unpublished).
[2] T.M. Klapwijk *et al.*, Physica B & C **109&110**, 1157 (1982).
[3] A.Yu. Kasumov *et al.*, Science **284**, 1508 (1999).
[4] C. Schoenenberger, Phys. Rev. Lett. (to be published).
[5] Y. Avishai *et al.*, Phys. Rev. **63**, 134515 (2001); Europhys. Lett. **54**, 640 (2001).
[6] Ya. Blanter and M. Büttiker, Phys. Rep. **336**, 1 (2000).
[7] Y. Avishai *et al.*, Europhys. Lett. **55**, 397 (2001).
[8] J. Nygard, D.H. Cobben, and D.E. Lindelof, Nature (London) **408**, 342 (2000).
[9] U. Gunsenheimer and A.D. Zaikin, Phys. Rev. B **50**, 6317 (1994).
[10] D. Averin and H.T. Imam, Phys. Rev. Lett. **76**, 3814 (1996).
[11] S.M. Cronenwett *et al.*, Science **281**, 540 (1998).
[12] D. Goldhaber *et al.*, Phys. Rev. Lett. **81**, 5225 (1998).
[13] P. Coleman, Phys. Rev. **29**, 3035 (1984).
[14] R. Fazio and R. Raimondi, Phys. Rev. Lett. **80**, 2913 (1998); **82**, 4950(E) (1999).
[15] P. Schwab and R. Raimondi, Phys. Rev. **59**, 1637 (1999).
[16] A.A. Clerk *et al.*, Phys. Rev. B **61**, 3555 (2000).
[17] Y. Meir and N.S. Wingreen, Phys. Rev. Lett. **68**, 2512 (1992).
[18] L.S. Borkowski and P.J. Hirschfeld, J. Low Temp. Phys. **96**, 185 (1994).
[19] L.I. Glazman and K.A. Matveev, JETP Lett. **49**, 659 (1989).
[20] A. Golub, Phys. Rev. B **54**, 3640 (1996).
[21] J.C. Guevas *et al.*, Phys. Rev. Lett. **82**, 4086 (1999).